JOURNAL OF CATALYSIS 60, 394–403 (1979)

Fischer–Tropsch Synthesis over Freshly Reduced Iron–Ruthenium Alloys

G. L. OTT,[1] T. FLEISCH,[2] AND W. N. DELGASS

School of Chemical Engineering, Purdue University, West Lafayette, Indiana 47907

Received December 26, 1978; revised May 21, 1979

Surface analysis of unsupported FeRu alloys was accomplished using x-ray photoelectron spectroscopy (XPS) and secondary ion mass spectrometry (SIMS) after the catalysts were reduced in flowing H_2 at 673 K for 4 h in a pretreatment chamber and introduced directly into the UHV instrument without exposure to the air. XPS lines show Fe and Ru to be metallic after reduction. Quantitative analysis of the first several layers using XPS shows enrichment of the surface region in Fe as expected. Analysis of the secondary ion emission as a function of composition shows a marked decrease in the Ru^+ emission from 97Ru3Fe compared to the pure Ru catalyst, suggesting alteration of the electronic properties of the surface upon addition of a small amount of Fe. Semiquantitative analysis of the uppermost layer using SIMS suggests greater Fe enrichment in the first layer than the average enrichment calculated from XPS for the first several layers. The initial activity and selectivity of the catalysts for Fischer–Tropsch synthesis were measured at 1 atm and 573 K in $3.3H_2 + CO$ at conversions below 3%. Selectivity to methane decreases through a minimum with increasing Fe content in the first layer. High propylene and ethylene yields were found for the alloy catalysts. A marked increase in the selectivity of the catalysts to propylene and, particularly, ethylene for 3Fe97Ru compared to pure Ru correlates with the sharp changes in SIMS yields.

INTRODUCTION

The wealth of literature related to Fischer–Tropsch synthesis which has appeared in the past few years indicates renewed interest in the technology of synthetic hydrocarbon production (e.g. (*1*, *2*)). Two of the more active metals for catalyzing the Fischer–Tropsch synthesis reaction are iron and ruthenium (*3*). Supported alloys of these two metals are known to possess unique catalytic properties for hydrocarbon synthesis, particularly high selectivity for propylene (*4*, *5*).

The goal of this research has been to characterize the surface of FeRu alloys in terms of composition, electronic properties, and purity and to correlate this information to kinetic behavior. First monolayer composition analysis is typically done by selective gas chemisorption, but this method is not useful in this case because both metals are very active for adsorption of most candidate gases. We have turned instead to surface analysis using X-ray photoelectron spectroscopy (XPS) and secondary ion mass spectrometry (SIMS).

The details of XPS have been described elsewhere (e.g., (*6*, *7*)). The spectrum is obtained by analysis of the kinetic energy of photoelectrons ejected from the surface of the catalyst during bombardment by X rays. Peak positions and areas provide qualitative analysis of all elements except hydrogen, information concerning the

[1] Present address: Amoco Oil Company, Naperville, Ill. 60540.

[2] Present address: Standard Oil Company, Naperville, Ill. 60540.

0021-9517/79/150394-10$02.00/0

chemical state of atoms in the surface region, and quantitative analysis of the surface with an accuracy of about 20%. XPS examines only the first several atomic layers of a sample because most photoelectrons ejected from deeper in the bulk are inelastically scattered before reaching the surface.

Secondary ion mass spectrometry measures the ions ejected from a solid surface during bombardment of the surface by incident ions in the kilo-electron volt range (*8*, *9*). Since the probability of particle ejection from the bulk is very low (*10*), SIMS examines only the first one or two atomic layers. In addition, multiatom clusters ions reflect local composition in regions approximately 10 Å in diameter and are believed, on the basis of kinematic calculations of particle ejection, to be formed just above the surface (*11*). Realization of the full potential of SIMS awaits further understanding of the particle ejection and ionization processes which generate secondary ions, but many of the uncertainties in SIMS can be removed by using XPS to aid in chemical characterization of the surface.

In order to correlate the catalytic behavior of the alloy surfaces with their structure and composition, kinetic measurements must be made. In this work, the alloys were prepared as unsupported powders with surface areas of 7 to 10 m^2/g (*12*), a convenient range for conventional kinetic analysis. Kinetic data were obtained at 1 atm and conversions below 3% in a fixed-bed, flow reactor system similar to that employed by Vannice (*3*).

We can expect from the literature for Fischer–Tropsch synthesis on Fe that bulk Fe can be transformed into Fe carbide during the reaction (*13–15*). In addition, Dwyer and Somorjai have shown that after 4 h at 573 K in 6 atm of $3H_2/CO$, the activity of an Fe foil for Fischer–Tropsch synthesis declined by a factor of 5 while a carbon layer sufficiently thick to eliminate

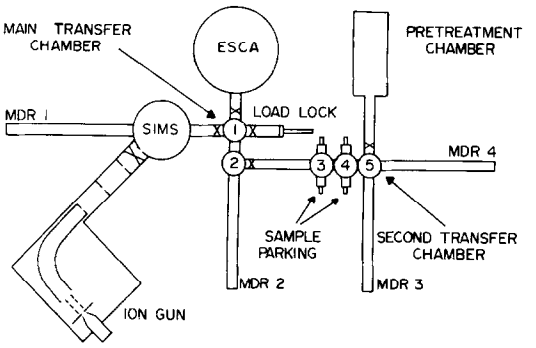

FIG. 1. Schematic of the SIMS/XPS apparatus (20). MDR = Magnetic drive rod.

Fe from an Auger spectrum formed over the surface (*16*). Our studies of the FeRu system have begun with SIMS/XPS analysis of the reduced and passivated alloy powders (*17*). In the present paper we report surface analysis of the hydrogen-reduced catalysts and studies of the effect of surface composition on the initial rates and selectivity for hydrocarbon synthesis at 1 atm pressure. A subsequent paper will deal with the alterations of the Fe, Ru, and FeRu alloy surfaces due to reactions during Fischer–Tropsch synthesis.

EXPERIMENTAL METHODS AND PROCEDURES

A. Surface Analysis

The overall XPS/SIMS instrument is shown schematically in Fig. 1 and is described in Refs. (*18–20*). The XPS measurements are made with a Hewlett–Packard 5950A electron spectrometer using monochromatic Al$K\alpha$ X rays. Linewidths on the order of 1.0 eV FWHM (Au $4f_{7/2}$) are typical and allow accurate determination of binding energies. The energy scale is calibrated by assigning 84.0 eV for the Au $4f_{7/2}$ binding energy.

The SIMS instrument is housed in a custom-designed Perkin–Elmer Ultek TNB-X ultrahigh vacuum (UHV) bell jar with a base pressure of 4×10^{-8} Pa. The mass filtered primary ion gun consists of a Danfysik 911A Sidenius-type hollow cath-

ode ion source, an extraction lens, and a 90° magnetic sector capable of unit resolution at 300 amu. For static SIMS experiments, the ion source can be operated in a pseudoelectron impact mode to deliver beam currents $<10^{-9}$ A/cm^2. The ion gun is connected to the UHV bell jar through three stages of differential pumping to maintain an operating pressure of 1×10^{-7} Pa during static SIMS experiments. To eliminate sputtering by neutrals, the 5-mm-diameter ion beam is deflected before striking the sample.

Both positive and negative ion high-mass SIMS spectra are taken with a Riber Q156 Quadrupole system which is capable of scanning between 2 and 800 amu at a resolution in excess of 800 ($m/\Delta m$). The quadrupole mass analyzer has 15-mm-diameter rods for high sensitivity and an off-axis spiraltron detector operated in the ion counting mode.

Samples are introduced into the system via a small volume, diffusion-pumped load lock. The transfer of samples within the system is accomplished with four magnetically driven transfer rods (MDR1–4) described in detail elsewhere (*20*). The reduced and passivated alloy powders are pressed into 7-mm-diameter by 1-mm-thick disks in a small hand-held press. Sample pellets are mounted on a cylindrical holder using a Hewlett–Packard copper sample blank, recessed for cylindrical disks, and a gold mask. Contamination of the sample due to copper migration is prevented by placing an aluminum disk under the sample. The holder is transferred to all points of the apparatus by right angle transfers between the different magnetic drive rods. Several samples can be stored in the system at once because of provisions to park samples when they are not being studied.

In addition to the XPS and SIMS analysis chambers, the apparatus includes a pretreatment chamber for the purpose of pretreating catalyst samples at 1 atm and up to 750 K, and then returning them to the vacuum system without exposure to air. The chamber, shown in Fig. 1, consists of a 35-mm-i.d. Pyrex tube connected to 70-mm (2.75 in.) conflat flanges via glass to metal seals. Replacement of this tube with one made of quartz would raise the maximum allowable pretreatment temperature considerably. Each end of the tube is connected to the rest of the system by flexible couplings to prevent unusual stresses in the glass. The system is pumped with a liquid-nitrogen-trapped, water-cooled, high-speed diffusion pump and is capable of a base pressure after bakeout of 7×10^{-7} Pa. Two chromel/alumel thermocouples, connected by a UHV feedthrough to a digital voltmeter, are used to measure the sample temperature. One is in the gas phase 2 mm from the sample. The other is in contact with the sample catching device. During treatment at atmospheric pressure, the two thermocouples read the same. After evacuation, the difference between the two is never larger than 5 K. Temperature measurements at various axial positions within the chamber show that the temperature variation in the sample region is less than

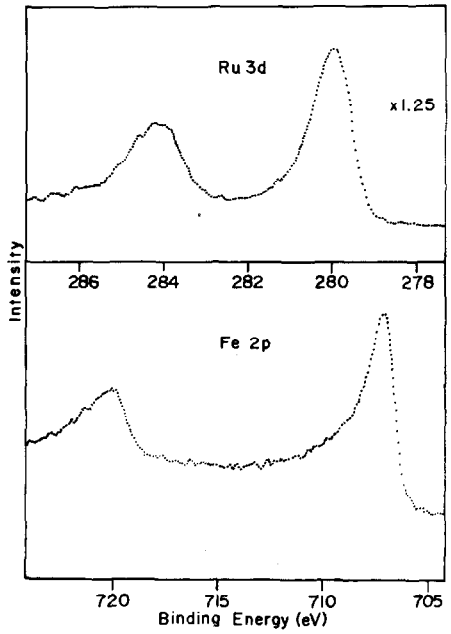

FIG. 2. XPS spectra of reduced 33Ru67Fe powder.

±5 K at 673 K and 100 cm³/min H_2/CO flow. Pressure is measured with a thermistor gauge at startup and a nude ionization gauge at low pressures. Reactant gases are introduced into the system through a Varian 13-mm valve mounted on a 70-mm conflat flange and the gases are all UHP quality from Matheson and are further purified by passage over a column of glass beads at 77 K.

The chamber pressure is typically at 1×10^{-3} Pa, 30 s after conclusion of the pretreatment (gas flow off, heater off, valve to pumps opened). The sample is usually introduced into the transfer system after 10 min when the pressure is $\sim 1 \times 10^{-4}$ Pa and the sample temperature is ~473 K. This procedure minimizes contamination of the sample from background gases.

B. Kinetic Analysis

The differential kinetic measurements are made on a separate apparatus (*21*). The gases available at the inlet are UHP H_2 (purified further with a Deoxo unit and molecular sieve trap), UHP He, and premixed $3.3H_2$/CO and $1H_2$/CO (purified by passage over a molecular sieve trap). The gases can be routed to three Pyrex reactors in parallel via several stainless-steel switching valves. The reactor U tubes are connected to the system with ultra-Torr O-ring seals and heated by a Techne fluidized sandbath controlled by a West on/off time proportioning controller. Temperature control is ±0.5 K and the sandbath insures good heat transfer away from the catalyst bed.

A Hewlett–Packard Model 5834A reporting gas chromatograph (gc) provides product analysis. This device includes a temperature-programmed Chromosorb 102 column, microprocessor control, digital integration, and a thermal conductivity detector. Water is removed from the product stream with a drierite trap prior to analysis. The carrier gas is He. The H_2 and CO peaks are not well resolved, but analysis of the CO_2 and C_1 to C_5 hydrocarbon products including unsaturated and isomerized products is done with high accuracy (±3%) and sensitivity (5 ppm). Absolute calibration of the gc is accomplished by running a certified calibration standard (Matheson) before each run. In preparation for kinetic measurements, catalysts were reduced in flowing H_2 for 4 h at 573 K. Kinetic runs were started by switching from H_2 to the reaction mixture at 573 K. Catalyst amounts varied from 0.2 to 1.5 g in order to maintain a conversion of ~1% in an ~100 cm³/min reactant gas flow.

Fe, Ru, and Fe–Ru powders were prepared from $RuCl_3 \cdot H_2O$ (Englehard) and $Fe(NO_3)_3 \cdot 9H_2O$ (Mallinckrodt) by hydrazine reduction as described previously (*12*, *17*, *22*).

RESULTS AND DISCUSSION

Iron and ruthenium form a continuous series of solid solutions with Fe substituted into the hcp Ru lattice above 24 mole% Ru in the bulk. Between 24.5 and 4.5% Ru, a two-phase region exists below 773 K. From 4.5 to 0% Ru in the bulk, the Ru atoms are substituted into the bcc Fe lattice. Except for pure Fe, all of the alloys investigated here were above 25% Ru in the bulk so the crystal structure of the materials is hcp (*23*).

A. Chemical State of the Reduced Catalysts

The surfaces of the reduced and passivated alloys have been shown previously (*17*) to consist of two phases, an Fe oxide phase and an FeRu alloy phase, as evidenced by XPS observation of Ru^0, Fe^0, Fe^{2+}, and Fe^{3+}. Reduction of the alloy catalysts at 673 K in 1 atm of H_2 for 4 h generated the XPS spectra shown in Fig. 2. As can be seen, Ru at 280.0 eV is zero valent as in the passivated catalysts, but now Fe, at 707.2 eV, is also zero valent as expected. A binding energy of 280.0 eV

TABLE 1

Bond Enthalpy Parameters for Fe and Ru (*31*)

Element	H_v (kcal/gmole)	Number of nearest neighbors (z)	Bond Enthalpy (kcal/gmole)
Fe (bcc)	96.68	8	24.17
Ru (hcp)	160.00	12	26.67

for Ru^0 is reported by Kim and Winograd (*24*). Brundle (*25*) and Kishi *et al.* (*26*) report values of 707.2 eV for Fe^0 when the 1*s* level of carbon is considered to be 284.0 eV. Pure Fe powder was also reduced completely by H_2 at 673 K. Examination of the O 1*s* region of the spectra typically showed O 1*s* to metal intensity ratios (normalized by photoelectric cross section (*27*)) of 0.1 to 0.2. These values correspond to roughly half a monolayer, assuming that an electron mean free path for inelastic collisions of 1.5 nm yields 30% of the detected signal from the first monolayer (*17*). Since C 1*s* overlaps with the Ru $3d_{\frac{3}{2}}$ line, the amount of carbon present was estimated by comparing the Ru $3d_{\frac{3}{2}}$/(Ru $3d_{\frac{3}{2}}$ + C 1*s*) intensity ratio to the value of 1.5 expected for the Ru $3d_{\frac{3}{2}}$/Ru $3d_{\frac{5}{2}}$ intensity ratio. Experimental values for the reduced surfaces were typically 4% greater than 1.5, indicating that the carbon coverage was below detectable limits. Since the cross-section ratio of Ru $3d_{\frac{3}{2}}$ to C 1*s* is 5.1 (*27*), a small change in the measured ratio can correspond to a significant amount of carbon. Thus we estimate the carbon coverage after reduction as less than 0.25 monolayers.

B. Surface Composition of the Reduced Catalysts

The possibility for surface enrichment in one of the components in a reduced binary alloy is well documented (*28–30*). As shown in Table 1, the bond enthalpy for Fe is lower than that for Ru (*31*). Thus surface enrichment in Fe is to be expected.

The procedure for measuring the surface composition of the reduced catalysts was to pretreat the samples in H_2 at temperatures exceeding 573 K for a minimum of 4 h. After the completion of the reduction period, the gas flow was interrupted, the pretreatment chamber evacuated, and the sample was introduced into the transfer system as described above. The time required to transfer the sample to the XPS chamber was usually about 5 min, so the sample was still cooling as it entered the X-ray photoelectron spectrometer.

Quantitative analysis by XPS was done using the most intense lines, $2p_{\frac{3}{2}}$ for Fe and $3d_{\frac{5}{2}}$ for Ru. A linear background was subtracted from the peaks to attempt to discount the inelastically scattered electrons. In contrast to the oxidized samples, the reduced samples have lineshapes which lend themselves to linear background subtraction (see Fig. 2). The spectral areas were obtained by computer integration and normalized for active counting time, horizontal scale, and photoelectric cross section (*27*). A final correction was required to account for the difference in energy of the two lines being investigated. Ru $3d_{\frac{5}{2}}$ has a binding energy of 280 eV and a kinetic

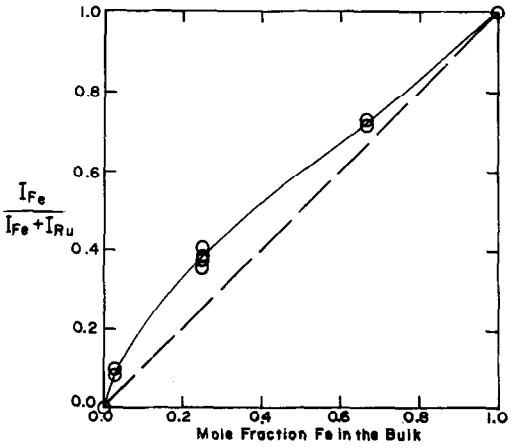

FIG. 3. XPS surface composition diagram for FeRu powders.

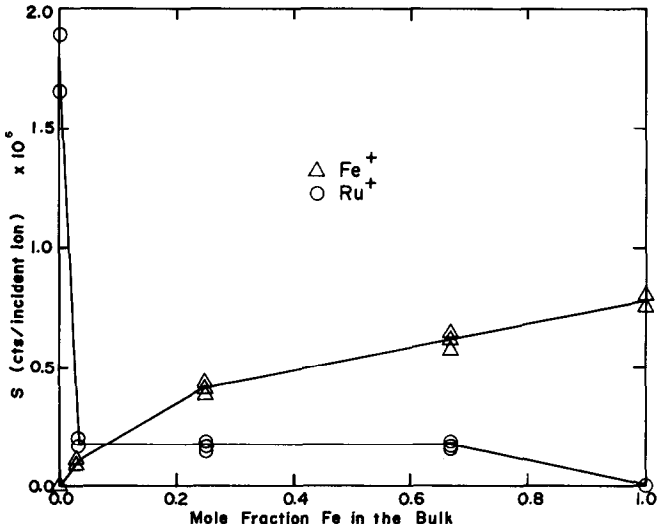

FIG. 4. Absolute Ru^+ and Fe^+ SIMS yields as a function of Fe bulk composition in FeRu powders.

energy of 1487 − 280 = 1207 eV. Fe $2p_{\frac{1}{2}}$ has a binding energy of 707 eV and a kinetic energy of 780 eV. In the region from 200 to 1000 eV kinetic energy, the mean free path (λ) varies as the square root of the kinetic energy (*32*). The normalized intensity of the Fe line must, therefore, be multiplied by $(1207/780)^{\frac{1}{2}}$ to account for the fact that the faster moving Ru electrons can escape from deeper within the sample and appear artificially more intense. With this normalization, $I_{Fe}/(I_{Fe} + I_{Ru})$ is the atom fraction of Fe in the surface region, assuming that the solid is homogeneous.

The results of the above calculations are presented in Fig. 3 and show surface enrichment in Fe as expected. Since the top layer contributes only 25 to 30% to a given XPS peak, enhanced enrichment in the first monolayer is a definite possibility. To gain a clearer picture of the composition of the first layer we turn to SIMS.

Although the quantitative understanding of the SIMS technique is not as well advanced as that of XPS, both experience and recent calculations (*10*) show that the sampling depth of the method is very low, with most of the secondary ions coming from the first layer. Semiquantitative analysis using SIMS has been discussed in the literature (*33*). A key experimental requirement is the use of low ion doses to avoid surface damage.

The secondary ion yield depends on the product of the particle ejection yield and the ionization probability. Gravimetric (total) sputter yields for Fe and Ru are reported as 0.8 and 1.0 atoms per incident ion, respectively (at 400 eV incident energy) (*34*). It is important to note, however, that these yields were not obtained under static conditions and that there may well be matrix effects on the yields which change with alloying. The fraction of emitted particles which are ionized is a function of both the atom being ionized and the nature of the surface, particularly its work function. Changes in the electronic properties of the surface due to chemisorption or oxidation can change ion yields by several orders of magnitude. Since no composition dependence of the small amount of surface contamination was noted in either SIMS or XPS, we assume that adsorption of background gas does not play a decisive role in determining relative ion yields as a function of composition in these experiments.

The absolute secondary ion yields of the Fe^+ and Ru^+ ions are presented in Fig. 4

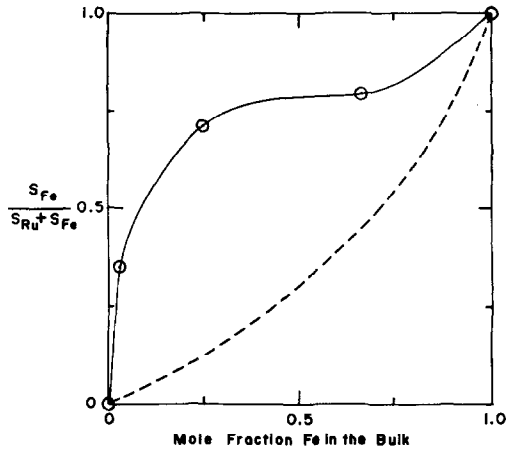

FIG. 5. Fractional SIMS yield of Fe as a function of Fe bulk concentration in FeRu powders. Dashed line is calculated assuming $S_{Fe}/(S_{Ru} + S_{Fe}) = X_{Fe}/(2.3X_{Ru} + X_{Fe})$.

as S (counts per incident ion) versus bulk atomic percentage Fe. Correction has been made for the $1/m^2$ dependence of the transmission function of the mass spectrometer on mass (*35*). Reproducibility of the results is excellent. The sharp decline in Ru^+ emission in the 97Ru3Fe alloy compared to pure Ru suggests a large surface enrichment in Fe. The Fe^+ yield is not high enough, however, to support a simple stoichiometric interpretation of Fig. 4. Some electronic or matrix effects on ion yields, particularly in the low Fe range, must be suspected. The yield ratio S_{Ru^+}/S_{Fe^+} for pure Ru versus pure Fe is 2.3. If electronic and matrix effects influence Fe and Ru equally, so that the ratio of relative probabilities of emission per surface atom is unchanged over the composition range, then the quantity $S_{Fe}/(S_{Ru} + S_{Fe})$ would equal $X_{Fe}/(2.3X_{Ru} + X_{Fe})$, where X_{Fe} and X_{Ru} are the surface atom fractions of Fe and Ru. This curve is compared to the experimental data for $S_{Fe}/(S_{Ru} + S_{Fe})$ in Fig. 5. The surface composition suggested by Fig. 5 is higher than would be predicted from XPS even if all the iron is in the first monolayer, but the suggestion of strong surface enrichment by Fe is intriguing, particularly in view of the kinetic findings discussed below.

C. Kinetic Analysis

Table 2 shows the initial synthesis activity of the different powders at 1 atm, $3.3H_2/CO$, and differential conversion. One can see that the overall rates on the alloy catalysts are roughly comparable while the rate over Fe is lower and that over Ru is higher. The CO turnover number is 10^{-2} s^{-1} for Ru at 538.5 K if the BET area is used for determining the number of surface metal atoms. Perhaps more interesting are the changes in selectivity with composition.

The selectivity analysis of the reduced Ru and 97Ru3Fe catalyst surfaces was accomplished by averaging the selectivity measurements over a 3-h period after introduction of the reactant mixture. This was possible because the selectivity did not vary with time within the experimental accuracy of the technique for these samples. For the Fe catalyst, the selectivity to C_n varied little with time so 3-h-averaged values were used. The olefin-to-paraffin ratio varied significantly, however. The 75Ru25Fe and 33Ru67Fe alloy samples showed a drastic change in selectivity with time on stream. Selectivity data for these two samples and olefin selectivity for Fe were measured by achieving reaction temperature in flowing hydrogen, introducing the $3.3H_2/CO$ mixture, and sampling after 15 min. The reasons for the change in

TABLE 2

Total Synthesis Rates

Sample	R^a ((gmole/min-gcat) $\times 10^5$)	Temperature (°K)
100Fe	0.41	574
67Fe33Ru	8.2	573
25Fe75Ru	7.8	574
3Fe97Ru	4.7	573
100Ru	21.5	573
100Ru	9.1	538.5

[a] R is the rate of CO conversion to C_1 to C_5 and CO_2.

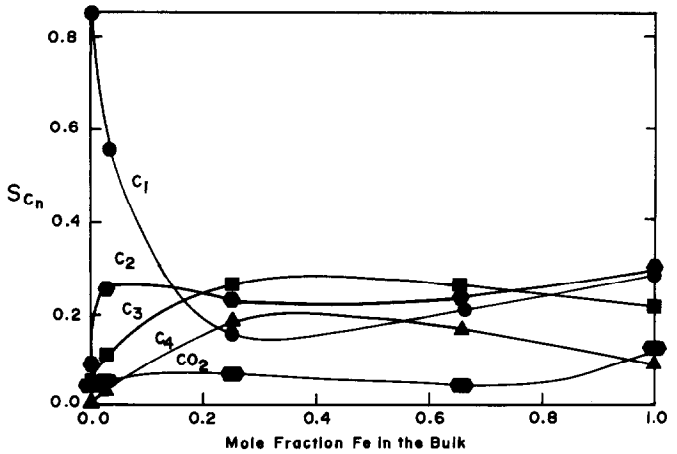

FIG. 6. Hydrocarbon selectivity in $3.3H_2/CO$ at 1 atm and 573 K for freshly reduced FeRu catalysts as a function of bulk composition. C_n indicates number of carbon atoms in the product molecule.

selectivity of the middle alloy catalysts will be discussed in a later paper.

Figure 6 shows the hydrocarbon selectivity of the freshly reduced alloy samples as a function of bulk composition. The selectivity values are reported on a carbon basis and can be thought of as the fraction of carbon atoms from reacted CO which are converted to a given product. The selectivity to methane decreases quickly, then goes through a slight minimum as the Fe content of the surface rises. Of special interest is the observation that the major changes in the selectivity of the catalysts occur below 30 atom% Fe in the bulk; the region which Fig. 5 shows to correspond to the major changes in surface composition. Compositions measured by XPS after reaction showed Ru/Fe ratios unchanged except for a small decrease for 33Ru67Fe.

The general features of Fig. 6 can be explained in terms of Fe enrichment of the surface, i.e., by the assumption that over much of the composition range the surface of FeRu alloys is largely Fe. Fe-Like behavior for unsupported 50Ru50Fe has also been reported by Urabe and Ozaki (*36*) for both ammonia synthesis and $^{14}N_2$–$^{15}N_2$ equilibration. Changes in olefin selectivity

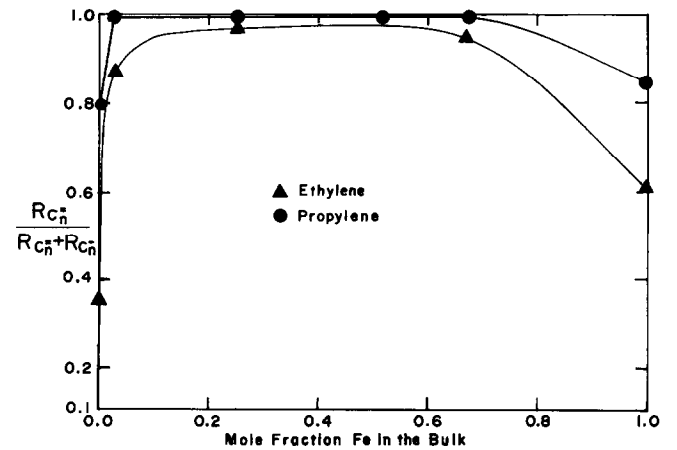

FIG. 7. Relative selectivity of FeRu catalysts to unsaturated products in $3.3H_2/CO$ at 1 atm and 573 K.

(Fig. 7) show, however, that Fe on the alloy surface is not identical to pure Fe.

Perhaps the most striking aspect of Figs. 6 and 7 is the large relative yield of ethylene at the 97Ru3Fe composition. The product distribution for this catalyst compared to pure Ru behaves as if the relative surface concentration of hydrogen had been lowered and the residence time of the carnon intermediates lengthened only enough to permit addition of one carbon to the chain. A lowering of the work function of Ru by introduction of 3% Fe is suggested by the low total secondary ion yield from 97Ru3Fe (see Fig. 4). By analogy to the promotional effect of K_2O on Fe Fischer–Tropsch catalysts (*37*), a lower work function can increase electron donation to CO, raising its heat of adsorption, and also suppress adsorption of $H^{\delta+}$. Thus it can account for the observed changes in hydrocarbon selectivity.

The selectivity changes at 97Ru3Fe show clearly that a surface with behavior intermediate between that of Ru- and Fe-covered alloy has been created. The SIMS spectra indicate that changes in both Fe_xRu_y ensemble distribution and electronic properties of the surface can be involved in determining the catalytic behavior. We also note that though high olefin yields have been found for supported FeRu (*4*, *5*), the selectivities are even higher for the unsupported metals and suggest influence of support interaction or particle size in the previous work. The drop in olefin selectivity, on reaching the 100% Fe side of the plot, may reflect a change from hcp to bcc structure as well as loss of the influence of Ru and, thus, invites further investigation.

CONCLUSIONS

XPS of the reduced catalysts shows Fe enrichment in the surface region. Semiquantitative interpretation of the SIMS data suggests that the first layer is greatly enriched in Fe. The catalytic behavior of the alloys as a function of composition shows a general trend in keeping with significant Fe enrichment of the surface but with special features in the high and low Fe content regions. The 97Ru3Fe alloy has unusually high C_2 yield with very high selectivity to ethylene. Although this surface could already have as much as 50% Fe, based on the SIMS analysis, its catalytic behavior is markedly different from that of the middle alloys whose surface could be 80–90% Fe. The changes in SIMS yield for 97Ru3Fe suggest that changes in work function as well as composition may be important in determining catalytic activity. The drop in olefin selectivity for pure bcc Fe versus the hcp alloys suggests that surface structure may also play a catalytic role.

ACKNOWLEDGMENTS

We are grateful to the National Science Foundation for support of this work by Grants MPS-7509308 and DMR76-00889A1. It is also a pleasure to thank R. L. Garten for information on preparing FeRu alloys, N. Winograd and W. E. Baitinger for enlightening discussions of several aspects of this research, and W. D. Kostka for obtaining the kinetic data on Ru powder.

REFERENCES

1. Mills, G. A., and Steffgen, F. W., *Catal. Rev.* **8**, 159 (1973).
2. Ponec, V., *Catal. Rev. Sci. Eng.* **18**(1),151 (1978).
3. Vannice, M. A., *J. Catal.* **37**, 449 (1975).
4. Vannice, M. A., Lam, Y. L., and Garten, R. L., *Amer. Chem. Soc. Div. Petrol. Chem. Prepr.* **23**, 495 (1978).
5. Lauderback, L., M. S. thesis, Purdue University, 1977.
6. Siegbahn, K., Nordling, C., Fahlman, A., Nordberg, R., Hamrin, K., Hedman, J., Johansson, G., Bergmark, T., Karlsson, S.-E., Lindgren, I., and Lindberg, B., *Nova Acta Regiae Soc. Sci. Upsal.* (4) **20** (1967).
7. Delgass, W. N., Hughes, T. R., and Fadley, C. S., *Catal. Rev.* **4**, 179 (1970).
8. Benninghoven, A., and Müller, A., *Surface Sci.* **39**, 416 (1973).
9. Benninghoven, A., *Surface Sci.* **53**, 596 (1975).
10. Harrison, D. E., Jr., Kelley, P. W., Garrison, B. J., and Winograd, N., *Surface Sci.* **76**, 311 (1978).

11. Garrison, B. J., Winograd, N., and Harrison, D. E., Jr., *J. Chem. Phys.* **69**, 1440 (1978).
12. Cusamano, J. A., and Garten, R. L., private communication.
13. Hofer, L. J. E., *in* "Catalysis," (P. H. Emmett, Ed.), Vol. 4, p. 373. Reinhold, New York, 1956.
14. Amelse, J. A., Butt, J. B., and Schwartz, L. H., *J. Phys. Chem.* **82**, 558 (1978).
15. Raupp, G. B., and Delgass, W. N., *J. Catal.* **58**, 337 (1979).
16. Dwyer, D. J., and Somorjai, G. A., *J. Catal.* **52**, 291 (1978).
17. Ott, G. L., Baitinger, W. E., Winograd, N., and Delgass, W. N., *J. Catal.* **56**, 174 (1979).
18. Shepard, A., Hewitt, R. W., Baitinger, W. E., Slusser, G. J., Winograd, N., Ott, G. L., and Delgass, W. N., "Quantitative Surface Analysis of Materials," ASTM STP 643, p. 187, Amer. Soc. for Testing & Materials, Philadelphia, 1978.
19. Fleisch T., Winograd, N., and Delgass, W. N., *Surface Sci.* **78**, 141 (1978).
20. Fleisch, T., Shepard, A. T., Ridley, T. Y., Vaughn, W. E., Winograd, N., Baitinger, W. E., Ott, G. L., and Delgass, W. N., *J. Vac. Technol.* **15**, 1756 (1978).
21. Kostka, W. D., M. S. thesis, Purdue University, 1978.
22. Garten, R. L. private communication.
23. Elliot, R. P., "Constitution of Binary Alloys: First Supplement," p. 431. McGraw-Hill, St. Louis, 1966.
24. Kim, K. S., and Winograd, N., *J. Catal.* **35**, 66 (1974).
25. Brundle, C. R., Chuang, T. J., and Wandelt, K., *Surface Sci.* **68**, 459 (1977).
26. Kishi, I., Ihida, K., and Ikeda, S., *Bull. Chem. Soc. Japan* **46**, 341 (1973).
27. Scofield, J. H., *J. Electron Spectrosc. Relat. Phenom.* **8**, 129 (1976).
28. Verbeek, H., and Sachtler, W. M. H., *J. Catal.* **42**, 257 (1976).
29. Bouwman, R., Toneman, L. H., and Holschar, A. A., *Surface Sci.* **35**, 8 (1973).
30. Williams, F. L., and Nason, P., *Surface Sci.* **45**, 377 (1974).
31. "Handbook of Chemistry and Physics." CRC Press, West Palm Beach, Fla., 1974.
32. Carlson, T. A., "Photoelectron and Auger Spectroscopy," p. 262. Plenum, New York, 1975.
33. Gerlach, R. L., and Davis, L. E., *J. Vac. Sci. Technol.* **14**, 339 (1977).
34. Oechsner, N., *Appl. Phys.* **8**, 185 (1975).
35. Dawson, P. H., *Int. J. Mass Spectrom. Ion Phys.* **21**, 317 (1976).
36. Urabe, K., and Ozaki, A., *J. Catal.* **52**, 542 (1978).
37. Dry, M. E., Shingles, T., Boshoff, L. J., and Oosthuizen, G. J., *J. Catal.* **15**, 190 (1969).